

Vibration Analysis of Orthotropic Triangular Nanoplates Using Nonlocal Elasticity Theory and Galerkin Method

A.R. Shahidi¹, S.H. Shahidi¹, A. Anjomshoei¹, E. Raeisi Estabragh^{2,*}

¹Department of Mechanical Engineering, Isfahan University of Technology, Isfahan, Iran

²Department of Mechanical Engineering, University of Jiroft, Jiroft, Iran

Received 29 June 2016; accepted 30 August 2016

ABSTRACT

In this article, classical plate theory (CPT) is reformulated using the nonlocal differential constitutive relations of Eringen to develop an equivalent continuum model for orthotropic triangular nanoplates. The equations of motion are derived and the Galerkin's approach in conjunction with the area coordinates is used as a basis for the solution. Nonlocal theories are employed to bring out the effect of the small scale on natural frequencies of nano scaled plates. Effect of nonlocal parameter, lengths of the nanoplate, aspect ratio, mode number, material properties, boundary condition and in-plane loads on the natural frequencies are investigated. It is shown that the natural frequencies depend highly on the non-locality of the nanoplate, especially at the very small dimensions, higher mode numbers and stiffer edge condition.

© 2016 IAU, Arak Branch. All rights reserved.

Keywords : Vibration analysis; Small scale effect; Nonlocal elasticity; Triangular nanoplate; Galerkin method.

1 INTRODUCTION

SUPERIOR mechanical, chemical and electrical properties of nanostructures cause their wide usage in different nano-devices such as nano-sensors, nano-actuators and nano-composites. For this reason, proper physical and mechanical analysis of these structures encompasses numerous advantages. After the invention of carbon nanotubes (CNTs) [1] and Graphene sheets (GS) [2], both experimental and theoretical studies on micro- and nano-engineering of nanostructures have been accelerated. However, experimental measurements are hard to reproduce and depend on the development of devices for manipulation of nano-sized objects. Numerical techniques based on semi-empirical approaches [3-4] such as molecular dynamic (MD) simulation, density functional theory (DFT), etc., provide a balance between accuracy and efficiency. Though these numerical methods produce results which are in good agreement with experimental results, a large amount of computational capacities are needed, especially when the number of atoms and bonds included in the system increase. Therefore, developing an appropriate computationally efficient mathematical model for the analysis of nanostructures is an important issue. Recently, continuum modeling of nanostructures has been the subject of much attention [5-10]. As the dimensions of a system reduce to the small scale, they become comparable to the inter-atomic or inter-molecular spacing of that system, and the material can no longer be treated as a continuum. Moreover, at small scale, the influence of long-range inter-atomic and inter-molecular cohesive forces on the static and dynamic properties tends to be significant and cannot be neglected. These are generally referred to as 'small scale' or 'size' effects. Classical continuum models are unable to account for quantum effects so there is a need to modify and upgrade the classical continuum theories to account for these effects.

*Corresponding author. Tel.: +98 34 43347069; Fax: +98 34 43347065.
E-mail address: e.raeisi@ujiroft.ac.ir (E. Raeisi Estabragh).

Modified continuum models benefit from the computational efficiency of classical continuum modeling and at the same time, produce accurate results comparable to the atomistic ones [11]. These models can be effectively used to simulate very small to very large systems. A well-known class of modified continuum models is based on the concept of the nonlocal elasticity theory introduced by Eringen [11-12]. In classical (local) continuum theories, it is assumed that stress state at a point in the continuum depends uniquely on strains at that point. In contrast, according to the nonlocal elasticity theory, it is assumed that stress state at a point depends on strains at all points of the continuum especially on those which are included in effective neighboring domains [12].

Vibration analysis of nanostructures is an important issue for proper design and use of many nano devices such as oscillators, sensors and actuators. There exist numerous studies on the use of nonlocal continuum modeling for vibration analysis of carbon nano-tubes and similar nano-beams [13-19]. In spite of the importance of structural analysis of nanoplates, few works have been reported on their theoretical modeling, as compared to the explorative studies on nano-beams and nanotubes. Triangular nanoplates belong to a class of nanoplates which have special application in vibrating nano-devices such as micro-electro-mechanical systems (MEMS) and nano-electro-mechanical systems [20]. Similar to CNTs, nanoplates possess superior mechanical properties [21-24]. Pradhan and Phadikar [25-27] reported transverse vibration analysis of embedded single- and multi-layered Graphene sheets and variational formulation for nonlocal elastic nanobeams. Vibration analysis of orthotropic Graphene sheets embedded in Pasternak elastic medium using nonlocal elasticity theory was reported by Pradhan and Kumar [28]. Aydogdu [29] investigated the effect of different boundary conditions on buckling and vibration of nonlocal plates by Levy method. Jomehzadeh and Saidi [30,31] studied three dimensional vibration of thick nanoplates and large amplitude vibration of multi-layered GSs. All of these works and other works conducted on nanoplate analysis [32-37] suggested that, size dependent Eringen's nonlocal elasticity theory should be included in continuum modeling of these structures for reaching accurate results.

In almost all of the studies conducted on frequency analysis of nanoplates, the shape of the nanoplate has received the less attention. Duan and Wang [38] reported exact solution for axisymmetric bending of circular Graphene sheets based on the nonlocal elasticity theory. Farajpour et al. [39] reported axisymmetric buckling of circular Graphene sheets using nonlocal continuum plate model. Babaie and Shahidi [40] studied small scale effect on vibration of quadrilateral multilayered GSs using the Galerkin method. Malekzadeh et al. [41] investigated thermal buckling and free vibration of orthotropic arbitrary straight-sided quadrilateral nanoplates using the nonlocal classical and first order plate theories. Moreover, Anjomshoa [42] investigated the buckling of embedded circular elliptical microplates and nanoplates via nonlocal elasticity theory.

It is recognized that the exact analytical solution for plate vibration are only available for a few plates with simple geometries like rectangle or circle nanoplates, under certain boundary and loading conditions. For frequency analysis of plates with arbitrary shape, numerical methods such as finite difference, finite element method (FEM) or finite strip method are usually used [43]. Although these methods provide a general framework for vibration analysis of nanoplate, they need large computational capacities. In FE analysis, for instance, due to the large number of discretization nodes, a large computational capacity is needed for an adequate approximation of the curved boundaries [44]. However, these inconveniences and approximations of boundaries via discretization do not arise when using the well-known meshless Galerkin method. Being a numerical approximate method, the Galerkin method eliminates the need for discretization by viewing the entire plate as a single super element.

In the present study, an orthotropic nonlocal continuum plate model based on classical plate theory is developed for frequency analysis of triangular nanoplates with arbitrary geometry. The principle of virtual work is used to derive the governing equation. Area coordinates in conjunction with the Galerkin method is used to provide a single super element that presents the whole nanoplate. Effects of the nonlocal parameter, nanoplate lengths, aspect ratio, mode number, material property, different boundary conditions and in-plane loads on non-dimensional frequencies are illustrated through tables and figures. The results show noticeable effect of non-locality on the frequencies of nano sized triangular plates.

2 FORMULATION

2.1 Geometric definitions

An arbitrary shaped triangular plate in the Cartesian coordinates system (x,y) can be easily mapped to a right angled triangular plate in the areal coordinates system (L_1, L_2) with the boundary equations being as $L_1=0$, $L_2=0$, and $L_1+L_2=1$, as shown in Fig. 1.

Referring to Fig.1, the areal coordinates of the point p , in general, are defined as:

$$L_1 = \frac{A_1}{A} \quad L_2 = \frac{A_2}{A} \quad L_3 = \frac{A_3}{A} \quad (1)$$

where, A_1 , A_2 and A_3 are the areas of sub-triangles shown in Fig. 1 and A is the area of the whole triangular plate. The three area coordinates are simply related to each other by the expression $L_1 + L_2 + L_3 = 1$. Also, the Cartesian and areal coordinates are related to each other through the following relations:

$$x(L_1, L_2) = \sum_{i=1}^N x_i L_i \quad (2a)$$

$$y(L_1, L_2) = \sum_{i=1}^N y_i L_i \quad (2b)$$

where, x_i and y_i ($i=1,2,3,\dots,N$) are the coordinates of vertices. After some mathematical manipulation, it can be shown that first-order and second-order derivatives in Cartesian coordinate system can be expressed based on the corresponding ones in the areal coordinate systems through the following relations:

$$\begin{Bmatrix} \frac{\partial^2}{\partial x^2} \\ \frac{\partial^2}{\partial y^2} \\ \frac{\partial^2}{\partial x \partial y} \end{Bmatrix} = [J_{22}]^{-1} \begin{Bmatrix} \frac{\partial^2}{\partial L_1^2} \\ \frac{\partial^2}{\partial L_2^2} \\ \frac{\partial^2}{\partial L_1 \partial L_2} \end{Bmatrix} - [J_{21}][J_{11}]^{-1} \begin{Bmatrix} \frac{\partial}{\partial L_1} \\ \frac{\partial}{\partial L_2} \end{Bmatrix} \quad (3a)$$

$$\begin{Bmatrix} \frac{\partial}{\partial x} \\ \frac{\partial}{\partial y} \end{Bmatrix} = [J_{11}]^{-1} \begin{Bmatrix} \frac{\partial}{\partial L_1} \\ \frac{\partial}{\partial L_2} \end{Bmatrix} \quad (3b)$$

In which, J_{ij} are mapping matrices defined as:

$$[J_{11}] = \begin{bmatrix} \frac{\partial x}{\partial L_1} & \frac{\partial y}{\partial L_1} \\ \frac{\partial x}{\partial L_2} & \frac{\partial y}{\partial L_2} \end{bmatrix} \quad (4a)$$

$$[J_{21}] = \begin{bmatrix} \frac{\partial^2 x}{\partial L_1^2} & \frac{\partial^2 y}{\partial L_1^2} \\ \frac{\partial^2 x}{\partial L_2^2} & \frac{\partial^2 y}{\partial L_2^2} \\ \frac{\partial^2 x}{\partial L_1 \partial L_2} & \frac{\partial^2 y}{\partial L_1 \partial L_2} \end{bmatrix} \quad (4b)$$

$$[J_{22}] = \begin{bmatrix} \left(\frac{\partial x}{\partial L_1}\right)^2 & \left(\frac{\partial y}{\partial L_1}\right)^2 & 2\left(\frac{\partial x}{\partial L_1}\right)\left(\frac{\partial y}{\partial L_1}\right) \\ \left(\frac{\partial x}{\partial L_2}\right)^2 & \left(\frac{\partial y}{\partial L_2}\right)^2 & 2\left(\frac{\partial x}{\partial L_2}\right)\left(\frac{\partial y}{\partial L_2}\right) \\ \left(\frac{\partial x}{\partial L_1}\right)\left(\frac{\partial x}{\partial L_2}\right) & \left(\frac{\partial y}{\partial L_1}\right)\left(\frac{\partial y}{\partial L_2}\right) & \left(\frac{\partial x}{\partial L_1}\right)\left(\frac{\partial y}{\partial L_2}\right) + \left(\frac{\partial y}{\partial L_1}\right)\left(\frac{\partial x}{\partial L_2}\right) \end{bmatrix} \quad (4c)$$

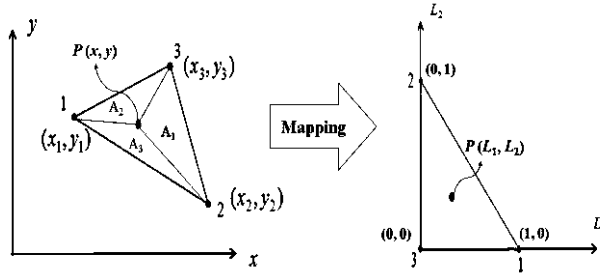


Fig.1
Mapping from Cartesian coordinate system to areal coordinate system.

2.2 Nonlocal classical plate theory

Schematic views of discrete and nonlocal continuum models of a triangular nanoplate are shown in Fig. 2. Cartesian coordinate system is chosen for deriving the governing equations. Origin is fixed at the center of the mid-plane. Since the nanoplate here is considered to be thin the classical plate theory (CPT) is adopted for the analysis.



Fig.2
Schematic views of a triangular nanoplate: (a) discrete model (b) nonlocal continuum model.

The displacement fields at time t according to CPT are written as:

$$u = u_0(x, y, t) - z \frac{\partial w}{\partial x}, \quad v = v_0(x, y, t) - z \frac{\partial w}{\partial y}, \quad w = w(x, y, t) \quad (5)$$

Here, u_0 , v_0 and w denote displacement of the point $(x, y, 0)$ along x , y and z directions, respectively. According to the Eringen [11-12] the nonlocal behavior of a Hookean solid can be introduced by the following differential constitutive equation:

$$\sigma^{(nl)} - (\alpha l_e)^2 \nabla^2 \sigma^{(nl)} = \sigma^{(l)} = S \epsilon \quad (6)$$

where, $\sigma^{(l)}$, $\sigma^{(nl)}$, S and ε denote local stress tensor, nonlocal stress tensor, elasticity tensor and strain tensor, respectively. For an orthotropic nonlocal plate model of nanoplate we have:

$$\sigma^{(l)} = \begin{Bmatrix} \sigma_{xx}^{(l)} \\ \sigma_{yy}^{(l)} \\ \sigma_{xy}^{(l)} \end{Bmatrix}, \quad \sigma^{(nl)} = \begin{Bmatrix} \sigma_{xx}^{(nl)} \\ \sigma_{yy}^{(nl)} \\ \sigma_{xy}^{(nl)} \end{Bmatrix}, \quad S = \begin{bmatrix} \frac{E_x}{1-\nu_x \nu_y} & \frac{\nu_x E_y}{1-\nu_x \nu_y} & 0 \\ \frac{\nu_y E_x}{1-\nu_x \nu_y} & \frac{E_y}{1-\nu_x \nu_y} & 0 \\ 0 & 0 & G_{xy} \end{bmatrix}, \quad \varepsilon = \begin{Bmatrix} \varepsilon_{xx} \\ \varepsilon_{yy} \\ 2\varepsilon_{xy} \end{Bmatrix} \quad (7)$$

In Eq. (6), $\alpha = e_0 l_i / l_e$ represents the nonlocal effect that depends on a characteristic length ratio l_i/l_e in which l_i is an internal characteristic length (lattice parameter, size of grain, granular distance, distance between C-C bonds) and l_e is an external characteristic length of system (wavelength, crack length, one size or dimension of the sample). The parameter e_0 is a constant appropriate to the material properties of the nanoplate and should be determined for each material independently [17]. It is obvious that $\alpha=0$ yields the well-known classical constitutive equation for elastic solids. Using the stress fields in Eq. (7), the Following stress and moment resultants are defined:

$$N = \begin{Bmatrix} N_{xx} \\ N_{yy} \\ N_{xy} \end{Bmatrix} = \int_{-\frac{h}{2}}^{\frac{h}{2}} \sigma^{(nl)} dz, \quad M = \begin{Bmatrix} M_{xx} \\ M_{yy} \\ M_{xy} \end{Bmatrix} = \int_{-\frac{h}{2}}^{\frac{h}{2}} z \sigma^{(nl)} dz, \quad (8)$$

where, h denotes the nanoplate's thickness. According to Eq. (6), the nonlocal effect enters through the constitutive relations. The principle of virtual work [27,45,46] is independent of the constitutive relations and then can be applied to derive the equilibrium equations for nonlocal plates herein. The motion in transverse direction gives:

$$\frac{\partial^2 M_{xx}}{\partial x^2} + 2 \frac{\partial^2 M_{xy}}{\partial x \partial y} + \frac{\partial^2 M_{yy}}{\partial y^2} + \frac{\partial}{\partial x} \left(N_{xx} \frac{\partial w}{\partial x} \right) + \frac{\partial}{\partial y} \left(N_{yy} \frac{\partial w}{\partial y} \right) + \frac{\partial}{\partial x} \left(N_{xy} \frac{\partial w}{\partial y} \right) + \frac{\partial}{\partial y} \left(N_{yx} \frac{\partial w}{\partial x} \right) + q_0 - m_0 \frac{\partial^2 w}{\partial t^2} + m_2 \left(\frac{\partial^4 w}{\partial t^2 \partial x^2} + \frac{\partial^4 w}{\partial t^2 \partial y^2} \right) = 0 \quad (9)$$

In which, m_0 and m_2 are, respectively, the mass per unit of area and the mass moment of inertia defined as:

$$m_0 = \int_{-\frac{h}{2}}^{\frac{h}{2}} \rho dz, \quad m_2 = \int_{-\frac{h}{2}}^{\frac{h}{2}} \rho z^2 dz \quad (10)$$

where, ρ denotes the nanoplate's density. Using Eqs. (6)-(10), the nonlocal moment resultants can be written in terms of displacements as:

$$M - \mu \nabla^2 M = -D \kappa \quad (11)$$

Here, $\mu = (e_0 l_i)^2$ is the nonlocal parameter, D is the bending rigidity matrix and κ the curvature matrix of the nanoplate defined as below:

$$D = \frac{h^3}{12} S, \quad \kappa = \left\{ \frac{\partial^2 w}{\partial x^2} \quad \frac{\partial^2 w}{\partial y^2} \quad 2 \frac{\partial^2 w}{\partial x \partial y} \right\}^T \quad (12)$$

Using Eqs. (8), (9) and Eq. (11) and assuming a modal solution as $w(x, y, t) = W(x, y)e^{i\omega t}$, the following general governing equation will be obtained for nonlocal plate in terms of displacements [26,28,29].

$$D_{11} \frac{\partial^4 W}{\partial x^4} + 2(D_{12} + 2D_{66}) \frac{\partial^4 W}{\partial x^2 \partial y^2} + D_{22} \frac{\partial^4 W}{\partial y^4} - (1 - \mu \nabla^2) \left[q_0 + m_0 \omega^2 W - m_2 \omega^2 \left(\frac{\partial^2 W}{\partial x^2} + \frac{\partial^2 W}{\partial y^2} \right) \right. \\ \left. + \frac{\partial}{\partial x} \left(N_{xx} \frac{\partial W}{\partial x} \right) + \frac{\partial}{\partial y} \left(N_{yy} \frac{\partial W}{\partial y} \right) + \frac{\partial}{\partial x} \left(N_{xy} \frac{\partial W}{\partial y} \right) + \frac{\partial}{\partial y} \left(N_{yx} \frac{\partial W}{\partial x} \right) \right] = 0 \quad (13)$$

where, W is a continuous function which represents the deflection of the nanoplate's mid-surface, q_0 is the applied transverse load and ω denotes the natural circular frequency.

3 SOLUTION PROCEDURE

The weighted residual statement corresponding to Eq. (13) can be written as:

$$\iint_R \left\{ D_{11} \frac{\partial^4 W}{\partial x^4} + 2(D_{12} + 2D_{66}) \frac{\partial^4 W}{\partial x^2 \partial y^2} + D_{22} \frac{\partial^4 W}{\partial y^4} - (1 - \mu \nabla^2) \left[q_0 + m_0 \omega^2 W - m_2 \omega^2 \left(\frac{\partial^2 W}{\partial x^2} + \frac{\partial^2 W}{\partial y^2} \right) \right. \right. \\ \left. \left. + \frac{\partial}{\partial x} \left(N_{xx} \frac{\partial W}{\partial x} \right) + \frac{\partial}{\partial y} \left(N_{yy} \frac{\partial W}{\partial y} \right) + \frac{\partial}{\partial x} \left(N_{xy} \frac{\partial W}{\partial y} \right) + \frac{\partial}{\partial y} \left(N_{yx} \frac{\partial W}{\partial x} \right) \right] \right\} \chi dx dy = 0 \quad (14)$$

where, χ denotes the weight function. By breaking the integral in Eq. (14), the following weak form will be obtained:

$$\iint_{\Omega} \Pi(x, y) dx dy + \int_{\Gamma} \Lambda(s) ds = 0 \quad (15)$$

where,

$$\Pi(x, y) = D_{11} \frac{\partial^2 W}{\partial x^2} \frac{\partial^2 \chi}{\partial x^2} + D_{12} \left[\frac{\partial^2 W}{\partial x^2} \frac{\partial^2 \chi}{\partial y^2} + \frac{\partial^2 W}{\partial y^2} \frac{\partial^2 \chi}{\partial x^2} \right] + D_{22} \frac{\partial^2 W}{\partial y^2} \frac{\partial^2 \chi}{\partial y^2} + 4D_{66} \frac{\partial^2 W}{\partial x \partial y} \frac{\partial^2 \chi}{\partial x \partial y} \\ - \omega^2 \left\{ m_0 \left[W \chi + \mu \left(\frac{\partial W}{\partial x} \frac{\partial \chi}{\partial x} + \frac{\partial W}{\partial y} \frac{\partial \chi}{\partial y} \right) \right] + m_2 \left[\frac{\partial W}{\partial x} \frac{\partial \chi}{\partial x} + \frac{\partial W}{\partial y} \frac{\partial \chi}{\partial y} + \mu \left(\frac{\partial^2 W}{\partial x^2} \frac{\partial^2 \chi}{\partial x^2} + 2 \frac{\partial^2 W}{\partial x \partial y} \frac{\partial^2 \chi}{\partial x \partial y} + \frac{\partial^2 W}{\partial y^2} \frac{\partial^2 \chi}{\partial y^2} \right) \right] \right\} \\ + N_{xx} \left[\frac{\partial W}{\partial x} \frac{\partial \chi}{\partial x} + \mu \left(\frac{\partial^2 W}{\partial x^2} \frac{\partial^2 \chi}{\partial x^2} + \frac{\partial^2 W}{\partial x \partial y} \frac{\partial^2 \chi}{\partial x \partial y} \right) \right] + N_{yy} \left[\frac{\partial W}{\partial y} \frac{\partial \chi}{\partial y} + \mu \left(\frac{\partial^2 W}{\partial x \partial y} \frac{\partial^2 \chi}{\partial x \partial y} + \frac{\partial^2 W}{\partial y^2} \frac{\partial^2 \chi}{\partial y^2} \right) \right] \\ + N_{xy} \left[\frac{\partial W}{\partial x} \frac{\partial \chi}{\partial y} + \frac{\partial W}{\partial y} \frac{\partial \chi}{\partial x} + \mu \left(\frac{\partial^2 W}{\partial x^2} \frac{\partial^2 \chi}{\partial x \partial y} + \frac{\partial^2 W}{\partial x \partial y} \frac{\partial^2 \chi}{\partial x^2} + \frac{\partial^2 W}{\partial y^2} \frac{\partial^2 \chi}{\partial x \partial y} + \frac{\partial^2 W}{\partial x \partial y} \frac{\partial^2 \chi}{\partial y^2} \right) \right] + q_0 \left[\chi - \mu \left(\frac{\partial^2 \chi}{\partial x^2} + \frac{\partial^2 \chi}{\partial y^2} \right) \right] \quad (16)$$

$$\begin{aligned}
\Lambda(s) = & \chi \left\{ \frac{\partial^3 W}{\partial x^3} (D_{11} + \mu(-m_2 \omega^2 + N_{xx})) n_x + \frac{\partial^3 W}{\partial x^2 \partial y} (D_{12} + \mu(-m_2 \omega^2 + N_{yy} + 2N_{xy} \frac{n_x}{n_y})) n_y + \frac{\partial^3 W}{\partial x \partial y^2} (D_{12} \right. \\
& + 4D_{33} + \mu(-m_2 \omega^2 + N_{xx} + 2N_{xy} \frac{n_y}{n_x})) n_x + \frac{\partial^3 W}{\partial y^3} (D_{22} + \mu(-m_2 \omega^2 + N_{yy})) n_y - \frac{\partial W}{\partial x} (-m_2 \omega^2 + N_{xx} \\
& + N_{xy} \frac{n_y}{n_x} + \mu(m_0 \omega^2)) n_x - \frac{\partial W}{\partial y} (-m_2 \omega^2 + N_{xy} \frac{n_x}{n_y} + N_{yy} + \mu(m_0 \omega^2)) n_y + \mu \left(\frac{\partial q_0}{\partial x} n_x + \frac{\partial q_0}{\partial y} n_y \right) \left. \right\} \\
& - \frac{\partial \chi}{\partial x} \left\{ \frac{\partial^2 W}{\partial x^2} (D_{11} + \mu(-m_2 \omega^2 + N_{xx} + N_{xy} \frac{n_y}{n_x})) n_x + \frac{\partial^2 W}{\partial x \partial y} (4D_{33} + \mu(-m_2 \omega^2 + N_{xx} + N_{xy} \frac{n_x}{n_y})) n_y \right. \\
& \left. \frac{\partial^2 W}{\partial y^2} (D_{12} n_x) + \mu q_0 \right\} - \frac{\partial \chi}{\partial y} \left\{ \frac{\partial^2 W}{\partial y^2} (D_{22} + \mu(-m_2 \omega^2 + N_{xy} \frac{n_x}{n_y} + N_{yy})) n_y + \mu \frac{\partial^2 W}{\partial x \partial y} (-m_2 \omega^2 + N_{xy} \frac{n_y}{n_x} \right. \\
& \left. + N_{yy}) n_x + \frac{\partial^2 W}{\partial x^2} (D_{12} n_y) + \mu q_0 \right\}
\end{aligned} \quad (17)$$

In which, n_x and n_y represent the components of the unit normal vector on the boundary Γ of the nanoplate shown in Fig. 2(a).

An approximate solution for the problem can be obtained by assuming an expression for the transverse deflection of the nanoplate mid-surface which satisfies the essential boundary condition at the edges as a summation with undetermined coefficients C_i [44]

$$W(L_1, L_2) = \sum_{q=0}^p \sum_{r=0}^q C_i \Phi_i(L_1, L_2) \quad (18)$$

In which, Φ_i are defined as:

$$\Phi_i = [L_1 L_2 L_3]^k \varphi_i(L_1, L_2) \quad (19)$$

Here, k is the power of the geometrical shape equation which is so obtained to satisfy the associated kinematic boundary conditions at the edges taking the values 0, 1 and 2 for free, simply supported and clamped edges, respectively. Also, φ_i are the polynomial functions of the form:

$$\varphi_i(L_1, L_2) = L_1^{q-r} L_2^r \quad (20)$$

where,

$$i = \frac{(q+1)(q+2)}{2} - r \quad (21)$$

In Eq. (18), p is the degree of polynomial set that may be increased until the desired accuracy is achieved. Using Eqs. (16,18-21) together with the Galerkin assumption (i.e. $x=\Phi_i$) the following simultaneous linear algebraic system of equations for both vibration and buckling problems will be yielded:

$$([K] - \beta_1 \lambda_\omega [M] + \beta_2 \lambda_b [B]) \{C\} = \{0\} \quad (22)$$

where, $[K]$, $[M]$ and $[B]$ are stiffness, mass and buckling matrices of the nanoplate, respectively, defined in Appendix A. The scalar indicators β_j take on: $\beta_1=1, \beta_2=0$ for free vibration analysis and $\beta_1=0, \beta_2=-1$ for buckling analysis, respectively. For the problem of vibration under the action of in-plane forces we have $\beta_1=1, \beta_2=+1$ in tensile loading case and $\beta_1=1, \beta_2=-1$ in compressive loading case. For simplicity and generality the non-dimensional parameters $\lambda_\omega = \omega a^2 (\rho h / D_{11})^{1/2}$ and

$\lambda_b = N_{xx} a^2 / D_{11}$ are defined which are, respectively, named as frequency parameter and load parameter. Eq. (22) is a standard eigen problem which can be solved for fundamental frequencies or buckling loads of orthotropic triangular nonlocal nanoplates. The corresponding eigenvector $\{C\}$ represents the associated vibration or buckling mode shape.

4 RESULTS AND DISCUSSIONS

4.1 Validation and convergence

In order to establish the validation of the current work, natural frequencies for an orthotropic square Graphene sheet with Young's modulus $E_x = 1765 \text{ GPa}$, $E_y = 1588 \text{ GPa}$, shear modulus $G_{xy} = 678.85 \text{ GPa}$, mass density $\rho = 2.3 \text{ gr/cm}^3$, Poisson's ratios $\nu_x = 0.3$, $\nu_y = 0.27$, and the thickness $h = 0.34 \text{ nm}$ are compared in Table 1. with the existing results in literature. It can be seen in this table that the results calculated by Eq. (22) for $p=10$, are in good agreement with those obtain by differential quadrature method (DQM) [28] and FEM [27]. Another comparison is also performed in Table 2. for natural frequencies associated with an isotropic local ($\mu=0 \text{ nm}^2$) right triangle nanoplate with Young's modulus $E_x = E_y = 1.06 \text{ TPa}$, mass density $\rho = 2.3 \text{ gr/cm}^3$, poisson's ratio $\nu_x = \nu_y = 0.3$, and the thickness $h = 0.34 \text{ nm}$ in both simply supported and clamped edge conditions. The results in Table 2. are presented for an isotropic right triangled plate. A desired agreement between the results obtained here and those reported by Kim and Dickinson [47] and Gorman [48] can be seen in this table. It is found from Tables 1. and 2 that a set of degree $p=10$ is sufficient for producing converged results and is used to generate all the other results presented herein.

Table 1

Convergence study of frequency parameter $\omega L^2 \sqrt{\rho / E_x h^2}$ for a orthotropic square Graphene sheet (CCC).

$\mu \text{ (nm}^2\text{)}$	Present Work			DQM [27]	FEM [28]
	$p=4$	$p=8$	$p=10$		
0	10.5951	10.5941	10.5941	10.5941	10.5533
1	9.5466	9.5457	9.5456	9.5446	9.5125
2	8.7535	8.7526	8.7525	8.7526	8.7242
3	8.1275	8.1267	8.1267	8.1267	8.1016
4	7.6177	7.6169	7.6169	7.6169	7.5949

Table 2

Results of convergence study of λ_m for local ($\mu=0$) triangular plate.

p	Aspect Ratio (b/a)				
	1	1.5	2	2.5	3
SSS					
4	49.3772	34.3846	27.8391	24.1904	21.9385
6	49.3482	34.2824	27.7600	24.1475	21.8565
8	49.3480	34.2810	27.7591	24.1445	21.8452
10	49.3480	34.2810	27.7591	24.1445	21.8448
Ref [47]	49.35	34.28	27.76	24.15	21.85
Ref [48]	49.35	34.28	27.76	24.08	21.84
CCC					
4	93.8094	65.5234	53.4702	46.9768	42.9629
6	93.7914	65.4596	53.4476	46.8930	42.7692
8	93.7896	65.457	53.4453	46.8844	42.7560
10	93.7893	65.4569	53.4449	46.8837	42.7553
Ref [47]	93.79	65.46	53.45	46.89	42.76
Ref [48]	93.86	65.46	53.45	46.88	42.76

4.2 Nonlocal effect

In this section the small scale effect on natural frequencies for different nanoplate geometries and mode numbers is investigated. The width of the nanoplate is varied between 5 nm and 30 nm and the range of aspect ratio is considered to increase from 0.5 to 3. The nonlocal parameter of the nanoplate is assumed to vary between $\mu=0 \text{ nm}^2$ and 4 nm^2 .

The effects of width length of clamped (CCC) right angled triangular nanoplate and the nonlocal parameter on the frequency parameter are shown in Fig. 3 for $b/a=2$. From this figure it is found that the natural frequencies of the nonlocal ($\mu \neq 0 \text{ nm}^2$) nanoplate are always smaller than those of local ($\mu=0 \text{ nm}^2$) nanoplate. In addition, in each value for the width, increasing the nonlocal parameter decreases the natural frequencies. The reason is that when the nonlocal parameter increases, the small scale effect increases and this leads to a reduction in the nanoplate stiffness by intensifying the mass matrix [25-31]. Also, as the width of nanoplate increases, the natural frequencies increase. This implies the size dependent nature of the nonlocal plate model that by increasing the external characteristic length of the nanoplate (here the length of width) the small scale effect decreases (the internal characteristic length is assumed to be unchanged). In fact, the size dependency in the nonlocal elasticity theory enters through the second term in the left side of the nonlocal constitutive equation in Eq. (6). It is seen that the dimensional parameters have a decreasing effect on the non-locality of nano-structures [25-31,42]. By further increasing in the width, the curves approach toward the local curve ($\mu=0 \text{ nm}^2$). Approximately for $a \geq 30 \text{ nm}$ the local theory assumptions can be employed with an admissible error. The relative errors due neglecting nonlocal effect for $a=10 \text{ nm}$ and $a=30 \text{ nm}$ with $\mu=4 \text{ nm}^2$, are obtained as %34.81 and %6.67, respectively. Here and afterwards, the relative error is defined as $(| \text{Local result} - \text{Nonlocal result} |) / (| \text{Local result} |) \times 100$.

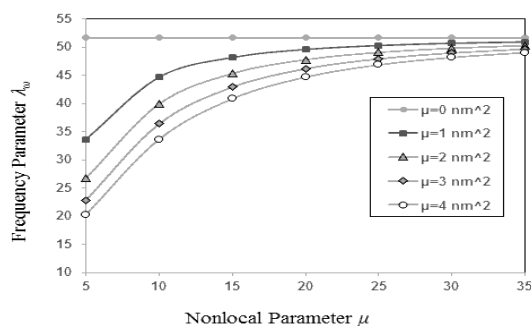


Fig.3
Variation of the natural frequency parameter with width of nanoplate for different nonlocal parameters (CCC).

To see the effect of aspect ratio on the vibration response of nonlocal triangular plate, the frequency parameter is plotted in Fig. 4 against the aspect ratios (b/a) for various nonlocal parameters. Here the width is taken as 10 nm . It is found from this figure that for smaller aspect ratio, the nonlocal effect is more prominent. An interpretation for such behavior is that for a specific value of width and nonlocal parameter, as the aspect ratio increases, the nanoplate become greater and this lead to a decrease in the small scale effect due to the previously discussed size dependency in nonlocal theory. The relative errors due neglecting small scale effect for ratios $b/a=1$ and $b/a=3$ with $\mu=4 \text{ nm}^2$ are obtained as % 44.98 and % 30.71, respectively. So, it can be concluded that nonlocal theory should be considered in small values of aspect ratio.

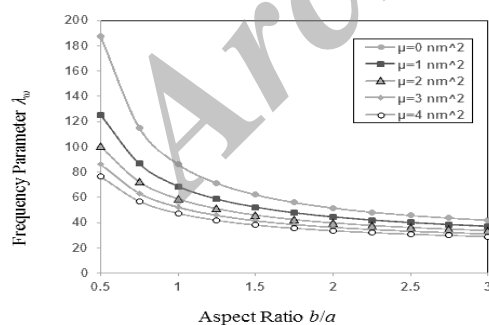


Fig.4
Variations of natural frequency parameter with aspect ratio for different nonlocal parameters (CCC).

To indicate the small scale effect in different modes, non-dimensional frequency parameters are plotted against the nonlocal parameter in Fig. 5 for the first four vibration modes. Here the width and aspect ratio are taken as $a=10 \text{ nm}$, $b/a=2.5$, respectively. It can be seen here that in all of the modes, as the nonlocal parameter increases, the frequency parameter decrease. Further, the nonlocal effect is more prominent in higher mode numbers. This is also true for circular and square nanoplate under uniform compression [25-31,39]. For the nonlocal parameter $\mu=4 \text{ nm}^2$ the relative error percent due neglecting nonlocal effect for the first and the fourth mode numbers are obtained as %32.41 and %51.75, respectively. These values indicate the importance of considering the nonlocal theory in higher vibration modes.

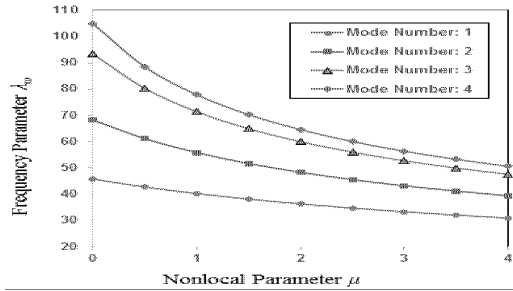


Fig.5
Variations of the first four frequency parameters with the nonlocal parameter (CCC).

4.3 Effect of material properties

An investigation is performed to account for the effect of anisotropy in the orthotropic case. For this purpose variations of the non-dimensional natural frequencies with various degrees of anisotropy i.e., E_y/E_x are presented in Fig. 6 for different nonlocal parameters. The figure shows that anisotropy has an increasing effect on the natural frequencies. Also, it is found that the difference between the nonlocal and local ones negligibly increases by the degree of anisotropy.

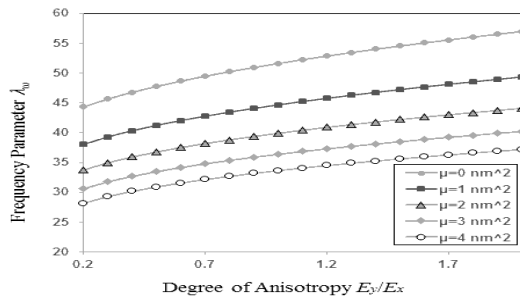


Fig.6
Variations of the natural frequency parameter with degree of anisotropy for different nonlocal parameters (CCC).

4.4 Effect of boundary condition

The effect of small scale on non-dimensional frequency parameter of triangular nanoplate is investigated in Fig.7 for different boundary conditions and nonlocal parameters. It is seen here that in both simply supported and clamped boundary conditions, as the nonlocal parameter increases the frequency parameter decreases. Further, it is found that the nonlocal effect is more prominent for clamped boundary condition. The relative error percent due neglecting small scale effect for simply supported a clamped edges with $b/a=1$ and $\mu=4 \text{ nm}^2$ are found to be % 40.58 and % 44.98, respectively. The increase in nonlocal effect for the stiffer supports was also reported for rectangular nanoplates by some researchers [28,29].

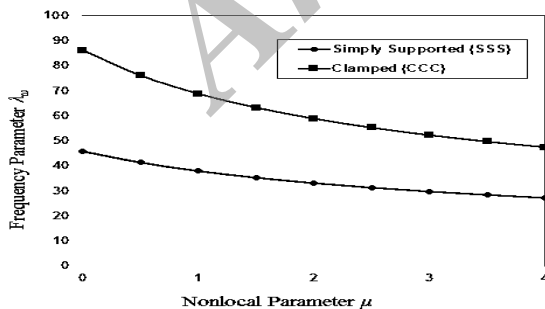


Fig.7
Variations of the natural frequency parameter with nonlocal parameter for different boundary conditions

4.5 Effect of in-plane loads

Since the governing equation in Eq. (13) also includes the influence of in-plane loads e.g. N_{xx} and N_{yy} , in this section the effect of such parameters on the natural frequencies of triangular nanoplate in the presence of small scale effect is investigated. Here, uniform in-plane load is assumed i.e. $N_{xx}=N_{yy}$ to be applied on the edges of a simply supported

right angled triangular nanoplate ($b/a=1$). Both tensile and compressive loading types are considered and the results are presented for different nonlocal parameters in Figs. 8 and 9, respectively. It is seen in Figs. 8 and 9 that as the nonlocal parameter increases the natural frequencies decrease for both tensile and compressive cases. In Fig. 8, it is seen that the tensile loads increases the natural frequencies of loaded nanoplate in comparison to the free standing one ($\lambda_b=0$). In fact, the tensile in-plane loading can be seen as an additional term added to the term related to the stiffness of the nanoplate in Eq. (22). On contrast, a compressive in-plane load decreases the natural frequency of the nanoplate which is clearly shown by Fig.9. By further increasing the compressive loads in Fig.9, the natural frequency of the nanoplate reaches zero where the nanoplate starts to buckle. For example, the curve $\lambda_b = -5$ in Fig. 9 for nonlocal parameter $\mu=4 \text{ nm}^2$ is close to zero because the critical in-plane load (buckling load) parameter for the nanoplate in this condition, i.e. $\mu=4 \text{ nm}^2$, is approximately $\lambda_b = -5.54$.

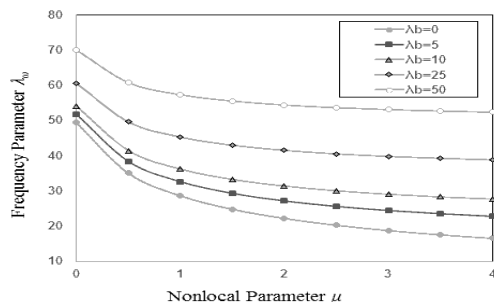


Fig.8

Variations of the natural frequency parameter with nonlocal parameter for different tensile in-plane loadings.

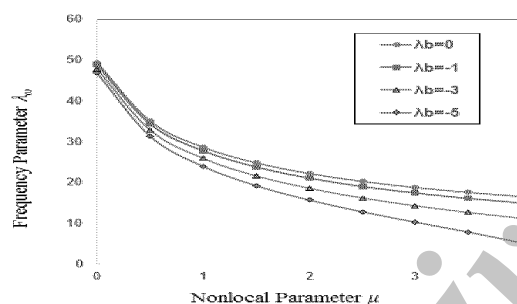


Fig.9

Variations of the natural frequency parameter with nonlocal parameter for different compressive in-plane loadings.

Finally, it should be noted that the current formulation based on CPT is valid for thin plate. For thick nanoplates, higher order plate theories must be considered to produce more accurate results [19,46,49]. A detailed study considering different plate theories for the bending and vibration analysis of nonlocal rectangular nanoplates is given by Aghababaei and Reddy [49] in which these theories are compared with each other and the domains of validation for each one is obtained. In Aghababaei and Reddy's work [49], Table 4., the error percent by using nonlocal CPT instead of nonlocal third order plate theory for $a/h=10$ is about %3. Thus the nonlocal classical plate theory can be desirably employed for the nanoplates with thickness to height ratio bigger than 10. It has to be mentioned that here the minimum length chosen for the nanoplate is 5 nm which means all the nanoplates analyzed herein are in the range $a/h > 10$.

5 CONCLUSIONS

In the present work, transverse vibration analysis of orthotropic triangular nanoplates at the small scale is carried out using the nonlocal CPT model. Based on the nonlocal theory, the governing equation for transverse vibration of orthotropic nano-plates is derived in the presence of in-plane loads and the Galerkin method is applied to find the solutions for frequencies. Areal coordinates system is employed to express the geometry of plates with arbitrary shape in a simple form, and then the interpolation functions are applied to form an assumed expression for displacement which satisfies the kinematic boundary conditions at the edges. The interpolation functions obviate the tedious task of choosing the form of the infinite series or trigonometric or algebraic functions to suit the conditions of support along the edges. Also, there is no need for mesh generation and thus large degree of freedoms which cause computational costs in other

numerical methods such as FEM and DQM. Results are presented for both simply supported and clamped nanoplates.

From the study the following conclusions can be drawn:

- The small scale has a decreasing effect on the frequencies of triangular nanoplates.
- Nonlocal effect becomes more prominent when the width of nanoplate decreases.
- The small scale effect decreases when the aspect ratio increases.
- Non-locality has greater influence on the frequencies in higher mode numbers.
- Frequency parameter increases by increasing the degree of anisotropy.
- The nonlocal effect is more prominent for clamped boundary condition.
- The in-plane load has considerable effect on the natural frequencies of nanoplate. Tensile in-plane loads strengthen the nanoplate stiffness and then increase the natural frequencies in contrast to the decreasing effect of small scale effect which is an asset. On the other hand the compressive in-plane loads together with the small scale effect both decrease the critical frequencies of the nanoplate system.

APPENDIX A

$$K_{ij} = \iint_R \left[D_{11} \frac{\partial^2 \Phi_i}{\partial x^2} \frac{\partial^2 \Phi_j}{\partial x^2} + D_{12} \left(\frac{\partial^2 \Phi_i}{\partial x^2} \frac{\partial^2 \Phi_j}{\partial y^2} + \frac{\partial^2 \Phi_i}{\partial y^2} \frac{\partial^2 \Phi_j}{\partial x^2} \right) + D_{22} \frac{\partial^2 \Phi_i}{\partial y^2} \frac{\partial^2 \Phi_j}{\partial y^2} + 4D_{66} \frac{\partial^2 \Phi_i}{\partial x \partial y} \frac{\partial^2 \Phi_j}{\partial x \partial y} \right] dx dy \quad (A.1)$$

$$M_{ij} = \iint_R \left\{ m_0 \left[\Phi_i \Phi_j + \mu \left(\frac{\partial \Phi_i}{\partial x} \frac{\partial \Phi_j}{\partial x} + \frac{\partial \Phi_i}{\partial y} \frac{\partial \Phi_j}{\partial y} \right) \right] + m_2 \left(\frac{\partial \Phi_i}{\partial x} \frac{\partial \Phi_j}{\partial x} + \frac{\partial \Phi_i}{\partial y} \frac{\partial \Phi_j}{\partial y} + \mu \left(\frac{\partial^2 \Phi_i}{\partial x^2} \frac{\partial^2 \Phi_j}{\partial x^2} + 2 \frac{\partial^2 \Phi_i}{\partial x \partial y} \frac{\partial^2 \Phi_j}{\partial x \partial y} + \frac{\partial^2 \Phi_i}{\partial y^2} \frac{\partial^2 \Phi_j}{\partial y^2} \right) \right] \right\} \quad (A.2)$$

$$B_{ij} = \iint_R \left[\bar{N}_x \frac{\partial \Phi_i}{\partial x} \frac{\partial \Phi_j}{\partial x} + \bar{N}_{xy} \left(\frac{\partial \Phi_i}{\partial x} \frac{\partial \Phi_j}{\partial y} + \frac{\partial \Phi_i}{\partial y} \frac{\partial \Phi_j}{\partial x} \right) + \bar{N}_y \frac{\partial \Phi_i}{\partial y} \frac{\partial \Phi_j}{\partial y} + \mu \left[\bar{N}_x \left(\frac{\partial^2 \Phi_i}{\partial x^2} \frac{\partial^2 \Phi_j}{\partial y^2} + \frac{\partial^2 \Phi_i}{\partial x \partial y} \frac{\partial^2 \Phi_j}{\partial x \partial y} \right) + \bar{N}_y \left(\frac{\partial^2 \Phi_i}{\partial y^2} \frac{\partial^2 \Phi_j}{\partial x^2} + \frac{\partial^2 \Phi_i}{\partial x \partial y} \frac{\partial^2 \Phi_j}{\partial x \partial y} \right) + \bar{N}_{xy} \left(\frac{\partial^2 \Phi_i}{\partial x^2} \frac{\partial^2 \Phi_j}{\partial x \partial y} + \frac{\partial^2 \Phi_i}{\partial x \partial y} \frac{\partial^2 \Phi_j}{\partial x^2} + \frac{\partial^2 \Phi_i}{\partial y^2} \frac{\partial^2 \Phi_j}{\partial x \partial y} + \frac{\partial^2 \Phi_i}{\partial x \partial y} \frac{\partial^2 \Phi_j}{\partial y^2} \right) \right] \right] dx dy \quad (A.3)$$

REFERENCES

- [1] Iijima S., 1991, Helical microtubules of graphitic carbon, *Nature* **354**: 56-58.
- [2] Stankovich S., Dikin D.A., Dommett G. H. B., Kohlhaas K., Zimney E., Stach E., Piner R., Nguyen S., Ruoff R., 2006, Graphene-based composite materials, *Nature* **442**: 282-286.
- [3] Mylvaganam K., Zhang L., 2004, Important issues in a molecular dynamics simulation for characterizing the mechanical properties of carbon nanotubes, *Carbon* **42**(10): 2025-2032.
- [4] Sears A., Batra R. C., 2004, Macroscopic properties of carbon nanotubes from molecular-mechanics simulations, *Physical Review B* **69**(23): 235406.
- [5] Sohi N., Naghdabadi R., 2007, Torsional buckling of carbon nanopeapods, *Carbon* **45**: 952-957.
- [6] Popov V. N., Doren V. E. V., Balkanski M., 2000, Elastic properties of single-walled carbon nanotubes, *Physical Review B* **61**: 3078-3084.
- [7] Sun C., Liu K., 2008, Dynamic torsional buckling of a double-walled carbon nanotube embedded in an elastic medium, *European Journal of Mechanics - A/Solids* **27**: 40-49.
- [8] Behfar K., Seifi P., Naghdabadi R., Ghanbari J., 2006, An analytical approach to determination of bending modulus of a multi-layered Graphene sheet, *Thin Solid Films* **496**(2): 475-480.
- [9] Wong E. W., Sheehan P. E., Lieber C. M., 1997, Nanobeam mechanics: elasticity, strength, and toughness of nano rods and nano tubes, *Science* **277**: 1971-1975.

- [10] Liew K. M., He X. Q., Kitipornchai S., 2006, Predicting nanovibration of multi-layered Graphene sheets embedded in an elastic matrix, *Acta Materialia* **54**: 4229-4236.
- [11] Eringen C., 1983, On differential equations of nonlocal elasticity and solutions of screw dislocation and surface waves, *Journal of Applied Physics* **54**: 4703-4710.
- [12] Eringen C., 2002, *Nonlocal Continuum Field Theories*, Springer, New York.
- [13] Wang Q., Wang C. M., 2007, The constitutive relation and small scale parameter of nonlocal continuum mechanics for modeling carbon nanotubes, *Nanotechnology* **18**(7): 075702.
- [14] Civalek Ö., Akgöz B., 2010, Free vibration analysis of microtubules as cytoskeleton components: nonlocal euler-bernoulli beam modeling, *Journal of Scientia Iranica* **17**(5): 367-375.
- [15] Civalek Ö., Çigdem D., 2011, Bending analysis of microtubules using nonlocal Euler–Bernoulli beam theory, *Applied Mathematical Modeling* **35**: 2053-2067.
- [16] Murmu T., Adhikari S., 2010, Nonlocal transverse vibration of double-nanobeam-systems, *Journal of Applied Physics* **108**: 083514.
- [17] Khademolhosseini F., Rajapakse R. K. N. D., Nojeh A., 2010, Torsional buckling of carbon nanotubes based on nonlocal elasticity shell models, *Computational Materials Science* **48**: 736-742.
- [18] Wang Q., Varadan V. K., 2006, Vibration of carbon nanotubes studied using nonlocal continuum mechanics, *Smart Materials and Structures* **15**: 659-666.
- [19] Reddy J. N., 2007, Nonlocal theories for bending, buckling and vibration of beams, *International Journal of Engineering Science* **45**: 288-307.
- [20] Luo X., Chung D. D. L., 2000, Vibration damping using flexible graphite, *Carbon* **38**: 1510-1512.
- [21] Zhang L., Huang H., 2006, Young's moduli of ZnO nanoplates: Ab initio determinations, *Applied Physics Letters* **89**: 183111.
- [22] Freund L. B., Suresh S., 2003, *Thin Film Materials*, Cambridge University Press, Cambridge.
- [23] Scarpa F., Adhikari S., Srikantha Phani A., 2009, Effective elastic mechanical properties of single layer Graphene sheets, *Nanotechnology* **20**: 065709.
- [24] Sakhaee-Pour A., 2009, Elastic buckling of single-layered Graphene sheet, *Computational Materials Science* **45**: 266-270.
- [25] Pradhan S. C., Phadikar J. K., 2009, Nonlocal elasticity theory for vibration of nanoplates, *Journal of Sound and Vibration* **325**: 206-223.
- [26] Pradhan S. C., Phadikar J. K., 2009, Small scale effect on vibration of embedded multilayered Graphene sheets based on nonlocal continuum models, *Physics Letters A* **37**: 1062-1069.
- [27] Phadikar J. K., Pradhan S. C., 2010, Variational formulation and finite element analysis for nonlocal elastic nanobeams and nanoplates, *Computational Materials Science* **49**: 492-499.
- [28] Pradhan S. C., Kumar A., 2010, Vibration analysis of orthotropic Graphene sheets embedded in Pasternak elastic medium using nonlocal elasticity theory and differential quadrature method, *Computational Materials Science* **50**: 239-245.
- [29] Aydogdu M., Tolga A., 2011, Levy type solution method for vibration and buckling of nanoplates using nonlocal elasticity theory, *Physica E* **43**: 954-959.
- [30] Jomehzadeh E., Saidi A. R., 2011, A study on large amplitude vibration of multilayered Graphene sheets, *Computational Materials Science* **50**: 1043-1051.
- [31] Jomehzadeh E., Saidi A. R., 2011, Decoupling the nonlocal elasticity equations for three dimension a vibration analysis of nano-plates, *Journal of Composite Structures* **93**: 1015-1020.
- [32] Salehipour H., Nahvi H., Shahidi A.R., 2015, Exact analytical solution for free vibration of functionally graded micro/nanoplates via three-dimensional nonlocal elasticity, *Physica E: Low-dimensional Systems and Nanostructures* **66**: 350-358.
- [33] Ansari R., Shahabodini A., Faghieh Shojaei M., 2016, Nonlocal three-dimensional theory of elasticity with application to free vibration of functionally graded nanoplates on elastic foundations, *Physica E: Low-dimensional Systems and Nanostructures* **76**: 70-81.
- [34] Kiani K., 2011, Small-scale effect on the vibration of thin nanoplates subjected to a moving nanoparticle via nonlocal continuum theory, *Journal of Sound and Vibration* **330**(20): 4896-4914.
- [35] Kiani K., 2011, Nonlocal continuum-based modeling of a nanoplate subjected to a moving nanoparticle, Part I: theoretical formulations, *Physica E: Low-dimensional Systems and Nanostructures* **44**: 229-248.
- [36] Kiani K., 2011, Nonlocal continuum-based modeling of a nanoplate subjected to a moving nanoparticle, Part II: parametric studies, *Physica E: Low-dimensional Systems and Nanostructures* **44**: 249-269.
- [37] Kiani K., 2013, Vibrations of biaxially tensioned-embedded nanoplates for nanoparticle delivery, *Indian Journal of Science and Technology* **6**(7): 4894-4902.

- [38] Duan W. H., Wang C. M., 2007, Exact solutions for axisymmetric bending of micro/nanoscale circular plates based on nonlocal plate theory, *Nanotechnology* **18**: 385704.
- [39] Farajpour A., Mohammadi M., Shahidi A. R., Mahzoon M., 2011, Axisymmetric buckling of the circular Graphene sheets with the nonlocal continuum plate model, *Physica E* **43**: 1820-1825.
- [40] Babaie H., Shahidi A.R., 2011, Vibration of quadrilateral embedded multilayered Graphene sheets based on nonlocal continuum models using the Galerkin method, *Acta Mechanica Sinica* **27**(6): 967-976.
- [41] Malekzadeh P., Setoodeh A. R., Alibeygi Beni A., 2011, Small scale effect on the vibration of orthotropic arbitrary straight-sided quadrilateral nanoplates, *Journal of Composite Structures* **93**: 1631-1639.
- [42] Anjomshoa A., 2013, Application of Ritz functions in buckling analysis of embedded orthotropic circular and elliptical micro/nano-plates based on nonlocal elasticity theory, *Meccanica* **48**: 1337-1353.
- [43] Shahidi R., Mahzoon M., Saadatpour M. M., Azhari M., 2005, Very large deformation analysis of plates and folded plates by finite strip method, *Advances in Structural Engineering* **8**(6): 547-560.
- [44] Liew K. M., Wang C. M., 1993, Pb-2 Rayleigh-Ritz method for general plate analysis, *Engineering Structures* **15**(1): 55-60.
- [45] Adali S., 2009, Variational principle for transversely vibrating multiwalled carbon nanotubes based on nonlocal Euler-Bernoulli beam model, *Nano letters* **9**: 1737-1741.
- [46] Reddy J. N., 1997, *Mechanics of Laminated Composite Plates, Theory and Analysis*, Chemical Rubber Company, Boca Raton, FL.
- [47] Kim S., Dickinson S. M., 1990, The free flexural vibration of right triangular isotropic and orthotropic plates, *Journal of Sound and Vibration* **141**(2): 291-311.
- [48] Gorman J., 1985, Free vibration analysis of right triangular plates with combinations of clamped – simply supported conditions, *Journal of Sound and Vibration* **106**(3): 419-431.
- [49] Aghababaei R., Reddy J.N., 2009, Nonlocal third-order shear deformation plate theory with application to bending and vibration of plates, *Journal of Sound and Vibration* **326**: 277-289.

Archive of SID